Separation Science and Technology
Publication details, including instructions for authors and subscription information:
http://www.informaworld.com/smpp/title~content=t713708471

Experimental Study of Extrachannel Zone Spreading in Sedimentation Field-Flow Fractionation

J. Janča[a]; F. Stehlík[a]; V. Slaví[a]
[a] INSTITUTE OF ANALYTICAL CHEMISTRY CZECHOSLOVAK ACADEMY OF SCIENCES, BRNO, CZECHOSLOVAKIA

To cite this Article Janča, J. , Stehlík, F. and Slaví, V.(1984) 'Experimental Study of Extrachannel Zone Spreading in Sedimentation Field-Flow Fractionation', Separation Science and Technology, 19: 10, 709 — 721
To link to this Article: DOI: 10.1080/01496398408060670
URL: http://dx.doi.org/10.1080/01496398408060670

SEPARATION SCIENCE AND TECHNOLOGY, 19(10), pp. 709-721, 1984

Experimental Study of Extrachannel Zone Spreading in Sedimentation Field-Flow Fractionation

J. JANČA, F. STEHLÍK, and V. SLAVÍK

INSTITUTE OF ANALYTICAL CHEMISTRY
CZECHOSLOVAK ACADEMY OF SCIENCES
611 42 BRNO, CZECHOSLOVAKIA

Abstract

The experimental arrangement for sedimentation field-flow fractionation comprises some specific parts that contribute to the spreading of the zone of the solute fractionated. These are, above all, the rotary passages and the injectors for charging the sample during the movement of the rotor. The zone spreading inside these critical junctions has not yet been studied. In this work, different designs of rotary passages providing for the solvent to enter the rotor and get out of it during movement, and for injecting the sample to be separated in different ways, are described. The extrachannel contribution was found to enhance the broadening of the zone of a monodisperse nonretained solute by 7–16.5% under given conditions, independent of the flow rate and rotation speed. The results obtained show that, with a proper design of the rotary passages, extrachannel spreading can be minimized to a level that does not substantially influence the results of fractionation.

INTRODUCTION

At present, sedimentation field-flow fractionation (SFFF) belongs among the most developed techniques of field-flow fractionation (FFF). SFFF was conceptually formulated already in Giddings' early work (*1*). Giddings et al. (*2*) have discussed the fundamental theoretical and experimental aspects of SFFF and, in a number of other papers, demonstrated experimentally the utility of SFFF for the separation of particles of diverse (including biological) origin. Kirkland et al. (*3, 4*) have improved above all the instrumentation of SFFF, which makes it possible to work with high centrifugal accelerations. Owing to its nature, SFFF is attractive, especially

0149-6395/84/1910-0709$3.50/0

in view of biological applications, and it is evident that other laboratories are beginning to use this technique (for a review, see Ref. 5).

With regard to its character and experimental equipment, SFFF differs somewhat from the other techniques of FFF. Despite the fact that the overall arrangement is still very similar to that used for liquid chromatography, there are differences stemming mainly from the necessity of introducing the sample to be fractionated into a moving rotor and bringing the separated fractions out of the rotor via special rotary passages. As long as it is not necessary to collect the separated fractions for further analysis, it would, in principle, be possible to build the detector cell directly into the rotor. However, this possibility was not studied in this work. Attention was paid to the arrangement of the sample-port system, so as to provide for the introduction of the sample in different ways when the rotor was moving.

The spreading of the zone of a monodisperse solute is an important characteristic of every separation. This spreading is usually described quantitatively by the height equivalent to a theoretical plate, H. A number of individual processes contribute to zone spreading in FFF, all having been theoretically substantiated and discussed in detail (*6*). The height equivalent to a theoretical plate has been expressed by the relationship

$$H = \sigma^2/L = 2D/R\bar{v} + w^2\bar{v}\chi/D + \Sigma H_i \qquad (1)$$

where σ is the standard deviation of the distribution function describing the resultant chromatogram, D is the diffusion coefficient of the solute, w and L are the distance between the walls of the channel and the length of the latter, respectively, and χ is a dimensionless quantity depending on retention R. The first term on the right-hand side of Eq. (1) expresses the contribution due to the longitudinal diffusion of the solute in the channel, and its value is usually negligible. The second term expresses the contribution of nonequilibrium processes taking place in the mobile phase in the channel, and it is directly proportional to the forward velocity of the solvent. Finally, the third term, ΣH_i, comprises the sum of all the other contributions to the overall value of H, i.e., such as those due to relaxation processes that take place during the separation in the channel, but also the spreading caused by the extrachannel parts of the separation system, such as the injection-port system, detector, all the connection capillaries, and the necessary auxiliary elements situated between the injector and detector. Hence, the contributions to zone spreading due to the separation system elements that do not directly bear upon the separation process are understood under the term "extra-channel spreading." In this work, attention will be given to the extrachannel zone spreading caused by the elements of the separation system, including the effect of the set-up of these elements in the overall separation system.

Alternatively, the number of theoretical plates, $N = L/H$, can be used to evaluate zone spreading.

EXPERIMENTAL

The overall separation system was composed of the individual elements, i.e., an injector (I), rotary passages (T), channel (C), and the detector cell (D). Four different arrangements, shown schematically in Fig. 1, were studied. With Arrangement A the sample was dosed by means of an injection syringe through a septum placed in the body of a rotary passage of Type T-I (see the following text) in the axis of rotation. After separation, the sample

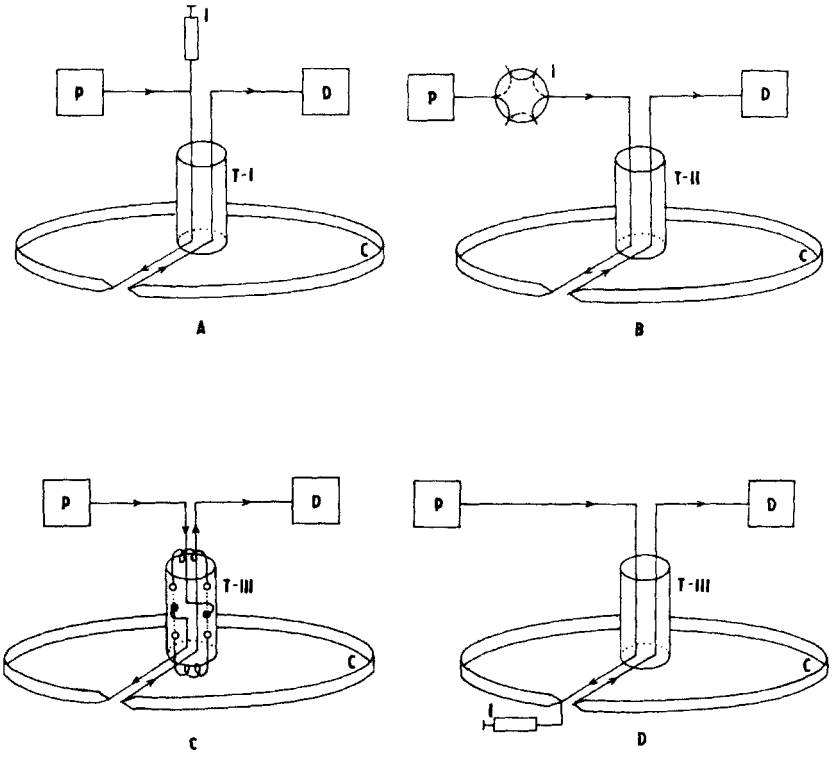

FIG. 1. Different arrangements of sample injection into the rotor in sedimentation field-flow fractionation: P = pump; D = detector; T-I, T-II, and T-III = rotary passages; C = channel, I = injector.

was passed to the detector via the concentric capillary of the rotary passage of Type T-I. This arrangement made it possible to introduce the sample during rotation. With Arrangement B, use was made of a rotary passage of Type T-II, and the sample was introduced by means of a six-port valve placed between the inlet of the rotary passage and the pump. The arrangement provided for also injecting the sample during rotation. In Arrangement C a rotary passage with the injector of Type T-III was used, also providing for the injection of sample directly into the channel during rotation. Finally, in Arrangement D the sample was introduced by an injection syringe through the septum situated directly at the channel inlet on the rotor circumference. In the latter case it was naturally possible to inject the sample only when the rotor was stopped. The solvent entered the channel at the injection port, and the separated sample left to enter the detector via the rotary passage of Type T-III, which will be described in the following text. Arrangements A and B are similar, the only difference being in the way of carrying out the sample injection. The six-port valve provides for a potentially higher degree of automation of sample injection. From the viewpoint of the scheme of the hydraulic circuit, overall Arrangements C and D are again very similar, but there is a substantial difference in their designs. In Arrangement C the entire sample-injection operation can be automated to a considerable degree.

Three types of rotary passage were constructed (designations T-I, T-II, T-III). The construction of rotary passage T-I, which was used with Arrangement A is shown in Figs. 2 and 3. The rotary passage (see Fig. 2) consists of two concentric capillaries (1) constituting a unit together with the rotor. The inlet and outlet parts of the capillaries reach into a nonrotating block (2). The rotating concentric capillaries (1) pass through stainless-steel rings (3) with rubber-ring sealings (4) placed in the nonrotating block (2). The whole system is pressed down axially by a guiding screw with a central opening and a septum for sample injection (5). The stainless-steel rings are connected by means of radial capillaries with the pump and detector cell. The prestressing of the sealing rings (4) is provided by the screw (5) that simultaneously serves as a guiding channel for the microsyringe needle when samples are introduced through the septum into the rotating inner capillary. The separated sample exits the channel via the outer concentric capillary and enters the detector.

Rotary passage T-II has been used with Arrangement B and is shown in Figs. 4 and 5. The body of the rotary passage (1) (see Fig. 4) constitutes part of the rotor. A part of the rotating body (1) is formed by a tightening screw (2) and stainless-steel collecting rings (3) provided with PTFE sealing O-rings, which allows the liquid to pass from the inner stationary capillary into the channel and to flow out of the channel via the outer concentric capillary.

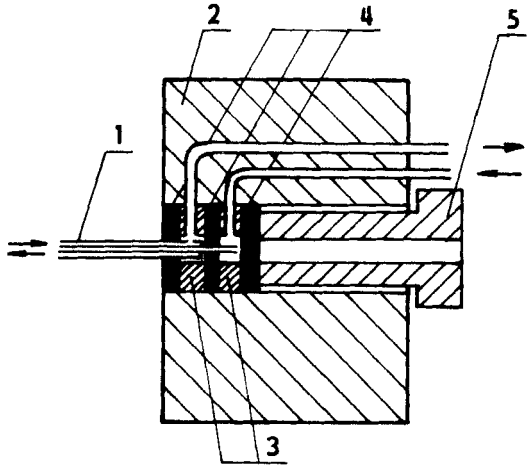

FIG. 2. Schematic representation of rotary passage T-I. For description, see text.

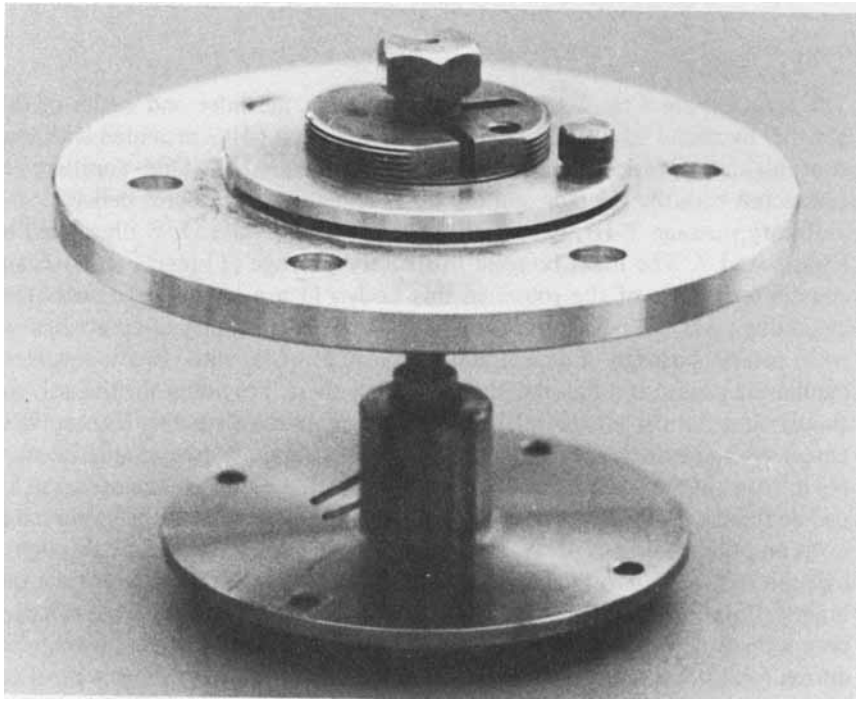

FIG. 3. Rotary passage T-I.

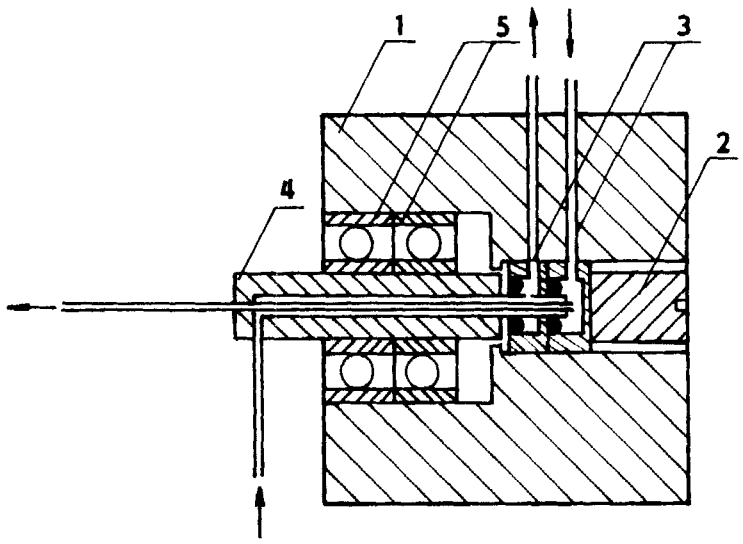

FIG. 4. Schematic representation of rotary passage T-II. For description, see text.

The stainless-steel rings (3) are connected with the inlet and outlet of the channel by radial capillaries. The nonrotating shaft (4) is provided with two concentric capillaries and is carried in bearings (5). One capillary is connected with the injector and the other leads to the detector cell.

Rotary passage T-III, used with Arrangements C and D, is illustrated in Figs. 6 and 7. The main body of this rotary passage (1) (see Fig. 6) again constitutes a part of the rotor. In this body (1) are located stainless-steel collecting rings (2) which are provided with PTFE sealing O-rings. Just as with rotary passage T-II, a stationary shaft (3) with two concentric capillaries passes through the stainless-steel rings, providing for the solvent supply and for the eluate to flow out and enter the detector. The solvent enters via the rotary passage and flows through axially traversable needles (4) into one of the capillary loops (5a, 5b). When the rotor is at rest, Loop 5a can be filled with the solution of the sample to be separated in the upper axial position of the needles (4). At the same time, the solvent can flow through a by-pass loop (5b) into the channel and out of it to enter the detector via the inner capillary of the rotary passage. In the central axial position the sample-port loop is closed, thus preventing the sample solution from flowing out during rotation; the solvent again flows through the by-pass. In this position the rotor is set in motion and, after the desired rotation has been reached, it is possible to connect the sample-port loop to the hydraulic circuit by shifting

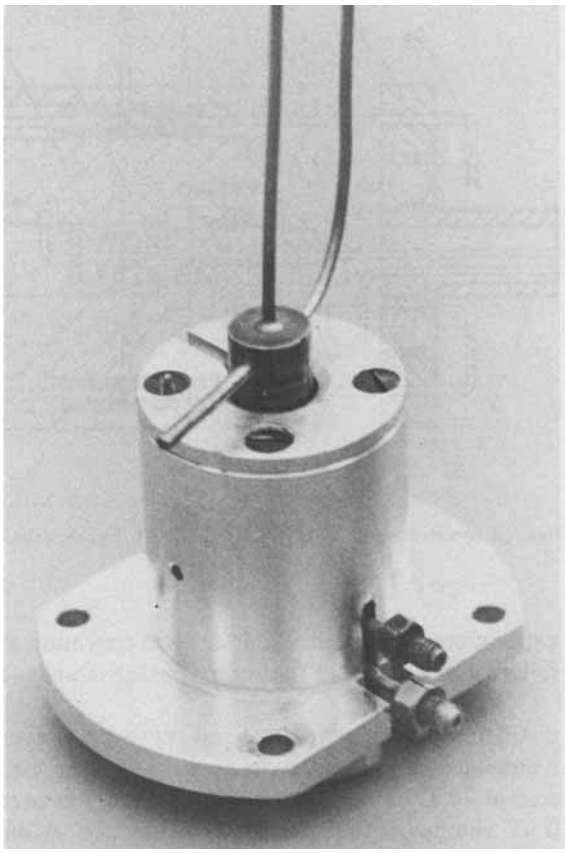

FIG. 5. Rotary passage T-III.

the needles down to the lower position and to simultaneously close the by-pass, thus introducing the sample into the channel. The separated sample leaves the rotor via the inner concentric capillary of the rotary passage. The axial movement of the sample-introduction needle system is actuated by means of a nonrotating holder (6) which is separated from the axially traversable rotating ring (7) by a ball bearing. In this ring (7) the needles (4) and the sampling loop (5a) are fixed.

The functional parts of all the three types of rotary passages, i.e., T-I, T-II, and T-III, have been designed so as to eliminate all dead volumes as much as possible, thus minimizing the undesirable extrachannel zone spreading. The individual parts of the rotary passages, their dimensions, materials, pre-stressing of the sealing rings, and the other constructional details were chosen

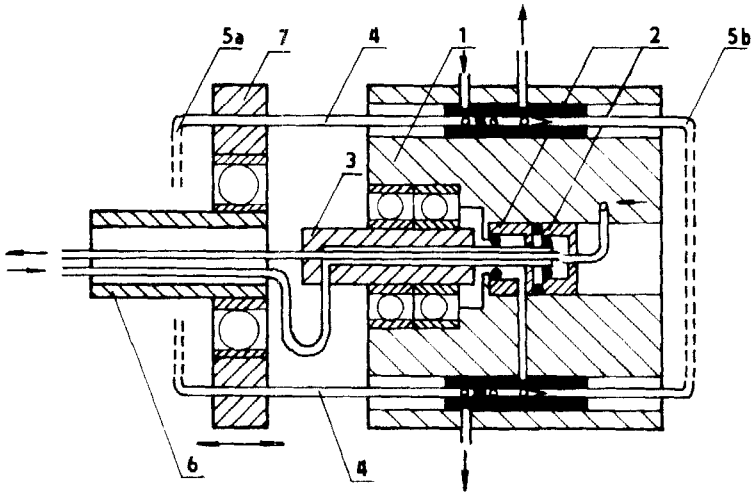

FIG. 6. Schematic representation of rotary passage T-III. For description, see text.

according to experimental experience in long-term operation and modified so as to ensure failureless function of the rotary passages under all operational conditions.

Degassed distilled water was used as a solvent to study extrachannel zone spreading. An aqueous solution of benzoic acid (Lachema, Brno, Czechoslovakia), saturated at 20°C and diluted 1:3 with water, was used as the model solute. 25–30 μL charges of the solution were injected. A differential flow-through UV detector operating at a wavelength of 254 nm (Development Workshops, Czechoslovak Academy of Sciences, Prague, Czechoslovakia) was employed for detection. As a pump, a high-pressure linear feeder (Laboratory Instruments, Prague, Czechoslovakia) was used. The rotor was equipped with a peripheral channel for SFFF and the centrifuge was electronically kept at constant speed with a 0.3% precision. All the measurements were carried out at ambient temperature (23–25°C) without any thermostatting of the separation system.

RESULTS AND DISCUSSION

Each rotary passage, T-I, T-II, and T-III, constitutes a certain dead volume. This dead volume is contributed by the individual volumes of the

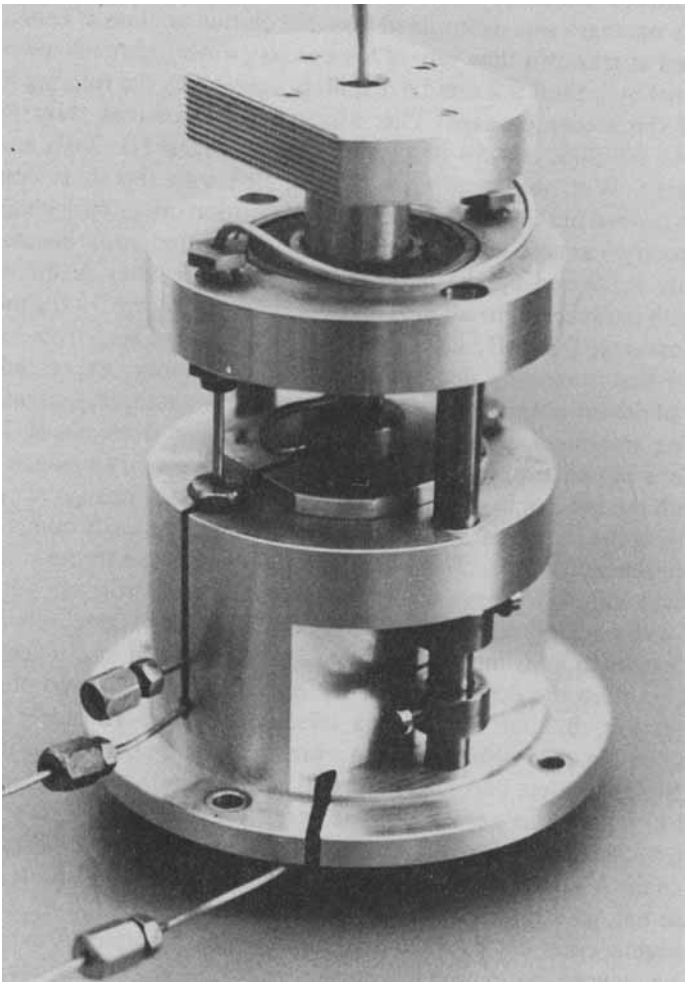

FIG. 7. Rotary passage T-III.

inlet and outlet capillaries, both rotating and stationary ones, the volumes between the sealing rings and the collecting rings of both the rotating and stationary parts, and/or the volumes of the sample-charging loops and the other constructional parts of the hydraulic path. The effective dead volume of the rotary passages was determined from the elution volume of benzoic acid, introduced at a known flow rate of the carrier (water) after having replaced the channel by a short 0.2 mm i.d. capillary connecting the rotating inlet and outlet of the rotary passage. The effective dead volumes were found to amount to 90, 200, and 54 μL with rotary passages T-I, T-II, and T-III, respectively. With the same arrangement, i.e., with the short connecting capillary instead of the channel, the effect of rotation on the spreading caused by the rotary passage was investigated. It was found experimentally that spreading, expressed by the number of theoretical plates N for instance, varied with the speed of rotation. This dependence is shown for the individual rotary passages, T-I, T-II, and T-III, in Fig. 8. It can be seen from Figs. 8(a) and 8(b) that spreading decreases (i.e., the efficiency, expressed as the number of the theoretical plates of the given rotary passages, increases) with increasing rotational speed within the limits from 0 to about 200–400 revolutions per minute. In the case of Fig. 8(c) (the rotary passage of Type T-III with the injector in Arrangement C), however, the change of spreading on changing the rotational speed is very small and practically commensurate with experimental errors. This effect is undoubtedly due to the mixing that takes place within the space where the rotating and nonrotating parts are in contact with each other, and/or where the initial translational movement of solvent passes to a regime in which rotational movement also takes place. It is apparent from the dependence of the efficiency on the speed of rotation, shown in Fig. 8, that this mixing effect contributes favorably to mass transport within dead volumes. From a practical point of view, it is important that this mixing effect become stabilized, i.e., at rotation speeds higher than about 400 revolutions per minute, the spreading due to the rotary passages no longer depends on the rotational speed within the limits of experimental errors. In the region of the flow rates studied, i.e., within 50–400 μL/min, the flow rate had no apparent influence on the mixing effect.

A suitable criterion, by means of which it is possible to evaluate the spreading caused by a given rotary passage in a certain experimental arrangement, is the ratio of the width of a zone having passed through the entire separation system, including the channel, rotary passage, injector, detector, and the connecting capillaries, to the width of the zone having passed through the channel only. It is assumed that the variances of the spreadings due to the individual elements of the system are additive, i.e.,

$$\sigma^2_{\mathrm{CITD}} = \sigma^2_{\mathrm{C}} + \sigma^2_{\mathrm{I}} + \sigma^2_{\mathrm{T}} + \sigma^2_{\mathrm{D}} = \sigma^2_{\mathrm{C}} + \sigma^2_{\mathrm{ITD}} \qquad (2)$$

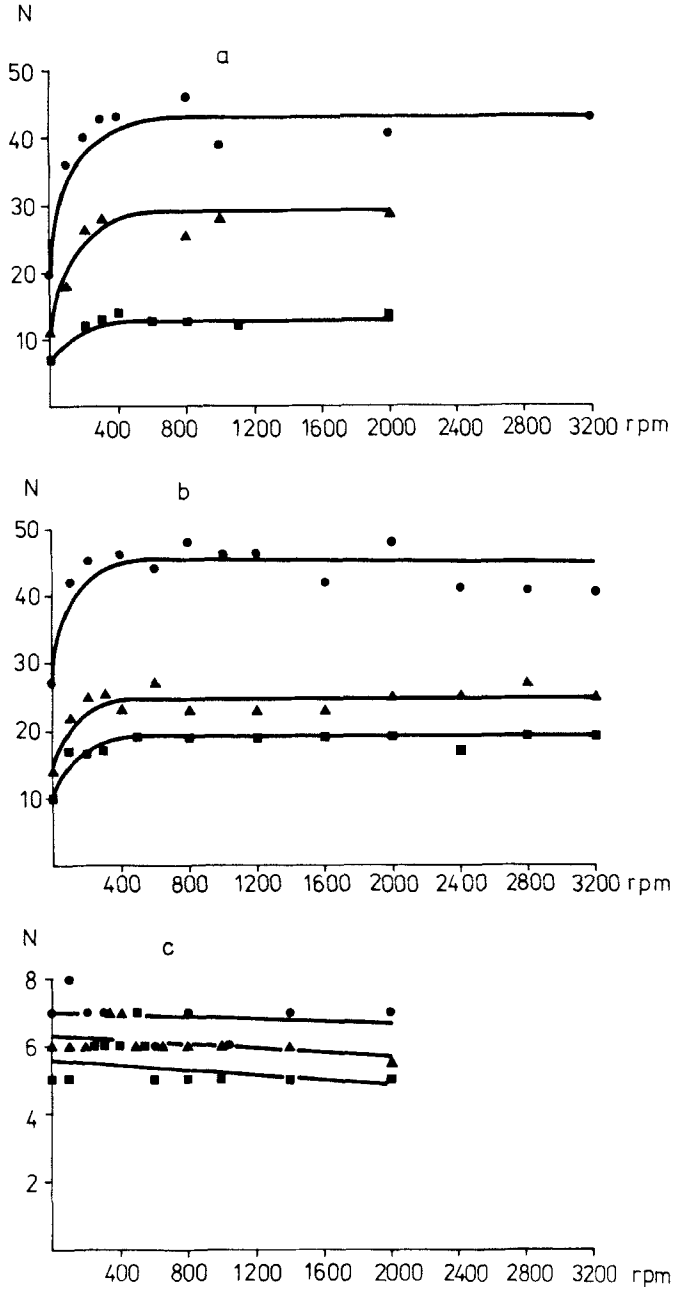

FIG. 8. Dependence of spreading expressed by the number of theoretical plates versus the number of revolutions per minute and on the flow rate for the individual rotary passages. (a) T-I, (b) T-II, (c) T-III; (●) 50 μL/min, (▲) 15 μL/min, (■) 400 μL/min.

where σ_C, σ_I, σ_T, and σ_D are the standard deviations of the spreading function caused by the channel, injector, rotary passage, and detector plus the connecting capillaries, respectively. The standard deviation of the spreading function that results after the zone has passed through the entire separation system, σ_{CITD}, can be determined by direct experimental measurement. The standard deviation σ_C can be calculated by Eq. (2), provided σ_{CITD} is already known and σ_{ITD} has been measured in such a way that the channel is replaced in the system by a short connecting capillary in which the spreading is negligible within the limits of experimental errors. In this way we determined experimentally the ratio σ_{CITD}/σ_C for all the types of rotary passage studied, i.e., T-I, T-II, and T-III, both at a standstill and during rotation. The speeds of rotation were high enough to keep N and the mixing effect constant. The measurements were accomplished for three different flow rates of the mobile phase: 50, 150, and 400 μL/min. The results of these measurements are summarized in Table 1. The following conclusions can be drawn from the σ_{CITD}/σ_C ratios found. With the extrachannel elements comprising the rotary passage of Type T-III, the zone spreading increased to the lowest degree. The average zone-width increase amounts to about 7%, without any significant effect of the rotation and/or mobile phase flow rate. Separation Arrangement A with rotary passage Type T-I is slightly worse from this point of view, the average increase of the zone width due to extrachannel elements being about 9%. Separation Arrangement B with rotary passage Type T-II appears to be worst in this comparison because the average increase of the zone width amounts to about 16.5% in this case. In the two latter cases the effects of both the rotation and flow rate are also insignificant. The differences found in the extrachannel contributions to zone spreading

TABLE 1
Change in the Zone Spreading Due to Extrachannel Elements of the Separation System under Different Experimental Conditions

Flow rate (μL/min)	Rotation speed (rpm)	σ_{CITD}/σ_C Separation system A	B	C
50	0	1.10	1.16	1.07
	>500	1.08	1.12	1.08
150	0	1.10	1.21	1.10
	>500	1.09	1.15	1.06
400	0	1.14	1.19	1.05
	>500	1.07	1.16	1.08

with different separation systems are due to differences in the dead volume of the individual rotary passages described above and to the different ways of performing sample injection. However, with regard to previous theoretical considerations (*7*), it is possible to state that the 7–16.5% zone-width increase due to extrachannel elements, as found experimentally for a monodisperse solute, is acceptable and will not strongly influence the results of the determination of size distribution of particles separated, even in cases of very narrow distributions. In addition to Separation Arrangements A, B, and C, Separation Arrangement D was studied. Rotary passage Type T-III was used in the latter system, but the sample was introduced while the rotor was at a standstill by an injection syringe through a septum situated directly at the channel inlet on the perimeter of the rotor. Hence, the rotary passage was utilized merely to lead the sample from the rotor into the detector. The measurements were carried out only at rotation speeds above 500 rpm. The values of the σ_{CITD}/σ_C ratio at three different flow rates, 50, 150, and 400 μL/min, were 1.04, 1.03, and 1.02, respectively. These results indicate an additional slight decrease in the contributions of the extrachannel elements of the separation system to overall zone spreading, so that the design of the individual rotary passages can still be somewhat improved in order to decrease their share in zone spreading. Further experimental work on this subject continues.

REFERENCES

1. J. C. Giddings, *Sep. Sci., 1*, 123 (1966).
2. J. C. Giddings, F. J. F. Yang, and M. N. Myers, *Anal. Chem., 46*, 1917 (1974).
3. J. J. Kirkland, W. W. Yau, W. A. Doerner, and J. W. Grant, *Ibid., 52*, 1944 (1980).
4. J. J. Kirkland, C. H. Dilks Jr., and W. W. Yau, *J. Chromatogr., 255*, 255 (1983).
5. J. Janča, K. Klepárnik, V. Jahnová, and J. Chmelík, *J. Liq. Chromatogr., 7*(S-1), 1 (1984).
6. M. E. Hovingh, G. H. Thompson, and J. C. Giddings, *Anal. Chem., 42*, 195 (1970).
7. J. Janča and K. Klepárnik, *J. Liq. Chromatogr., 5*, 193 (1982).